Thermochimica Acta 497 (2010) 117–123

Contents lists available at ScienceDirect

Thermochimica Acta

journal homepage: www.elsevier.com/locate/tca

Thermal and FTIR analysis of the miscibility and phase behaviour of poly (isobutyl methacrylate-co-4-vinylpyridine)/poly (styrene-co-acrylic acid) systems

Assia Siham Hadj-Hamou, Abderrahmane Habi, Said Djadoun*

Laboratoire des Matériaux Polymères, Faculté de Chimie, Université des Sciences et de la Technologie Houari Boumediene, B.P. 32, El Alia, Algiers 16111, Algeria

ARTICLE INFO

Article history:
Received 11 January 2009
Received in revised form 26 August 2009
Accepted 27 August 2009
Available online 2 September 2009

Keywords:
Miscibility
Hydrogen bonding
Phase behaviour
Poly (styrene-co-acrylic acid)
Poly (isobutyl methacrylate-co-4-vinylpyridine)

ABSTRACT

The miscibility and phase behaviour of poly (isobutyl methacrylate-co-4-vinylpyridine) containing 20 mol% of 4-vinylpyridine (IBM4VP20) and poly (styrene-co-acrylic acid) containing 27 or 32 mol% of acrylic acid (SAA27 or SAA32) mixtures were investigated by DSC, TGA and FTIR spectroscopy in the 25–180 °C temperature range. The results showed that sufficient specific carboxyl–pyridine hydrogen bonding interactions occurred between these copolymers and led to miscible blends as cast from THF and to inter-polymer complexes of significantly improved thermal stability when butan-2-one is the common solvent. The self-association effect on the inter-polymer interactions was evidenced by the decrease of complexation yields, observed when the carboxylic content is increased above 27 mol% as with SAA32.

The trend of phase behaviour predicted by a thermodynamic analysis of the specific interactions of hydrogen bonding type that occurred between the two components of the SAA27/IBM4VP20 blends, neglecting the weak carboxyl–ester interactions and the functional group accessibility effect, carried out using the Painter–Coleman association model that considers the screening effects, is in a fair agreement with the experimental results. Moreover an LCST is predicted to occur at relatively high temperature.

1. Introduction

The elaboration of novel materials with a wide range of properties by blending polymers is still of interest [1–5]. The miscibility of a polymer blend is a very important and desirable property in the elaboration of new polymer materials with optimum properties. The miscibility of most reported pairs of polymers, mainly due to the contribution of sufficient specific interactions that occurred between them, has been largely studied [6–11]. Such miscible blends are however expected to have lower critical solution temperature (LCST) behaviour and may phase separate in some cases at temperatures that affect their processing.

In order to improve some of the undesirable properties of poly (isobutyl methacrylate) PIBMA or poly (isobutyl methacrylate-co-4-vinylpyridine) IBM4VP, mixing these latter with poly (styrene-co-acrylic acid) (SAA) may also offer an opportunity to elaborate various materials and explore some of their interesting new properties.

Previous studies showed however that, though specific interactions between the carboxylic groups of SAA (up to SAA32) and the ester groups of PIBMA are expected to occur, mainly due to steric effect, SAA and PIBMA are immiscible [12,13] as evidenced by DSC.

Poly (styrene-co-acrylic acid) (SAA) and poly (isobutyl methacrylate-co-4-vinylpyridine) (IBM4VP) copolymers of various compositions were synthesized, characterized and used to investigate qualitatively the transition from immiscibility to miscibility and to the formation of miscible blends and inter-polymer complexes using THF or butan-2-one as the common solvent [13,14]. Such phenomena depend mainly on the nature of the solvent, densities of functional groups and their accessibility to develop specific intermolecular interactions.

Dadmun et al. [15,16] reported the concept of improving the miscibility of pairs of polymers by introducing and optimizing the extent of intermolecular interactions between the two components of the blends and correlated this extent to the phase behaviour. These authors [16] also correlated the optimum amount of intermolecular hydrogen bonding developed in a polymer blend to optimum improved properties of corresponding materials.

We have previously applied this concept [17] for poly (styrene-co-acrylic acid)/poly (styrene-N,N-dimethylacrylamide) blends (SAA/SAD) and found an optimal standard inter-association equilibrium constant for a copolymer composition of about 27 mol% of acrylic acid.

The optimization of the specific inter-polymer interactions in a polymer blend depends on several factors. Based on reported experimental results [17], we will in a first part of this contribution, investigate the miscibility and the specific interactions that occurred between the components of the SAA27/IBM4VP20 system

---

* Corresponding author.
E-mail address: matpolylab@yahoo.fr (S. Djadoun).

0040-6031/$ – see front matter © 2009 Elsevier B.V. All rights reserved.
doi:10.1016/j.tca.2009.08.015

Table 1
Polymer characteristics.

Sample	$[\eta]$ (dl/g)	M_n ($\times 10^{-4}$ g/mol)	M_w ($\times 10^{-4}$ g/mol)	$I = M_w/M_n$	DP	Tg (°C)
IBM4VP20	1.20	–	–	–	800	86.0
SAA27	–	10.00	14.6	1.46	1000	130.0
SAA32	–	2.47	4.27	1.73	800	134.0

M_w: weight average molecular weight, M_n: number average molecular weight, $I = M_w/M_n$: polydispersity index, DP: degree of polymerization, Tg: glass transition temperature.

by FTIR spectroscopy and DSC. The extent of hydrogen bonding in these blends will be then quantified and correlated to their thermal stability.

The Painter–Coleman association model [18] has been widely used to describe the phase behaviour of binary polymer blends involving strong specific interactions of hydrogen bonding type with reasonable agreement with the experiment [19–21].

In a second part of the present contribution, a thermodynamic analysis of hydrogen bonding in this system will be carried using the Painter–Coleman association model that also considers the polymer chain connectivity effect and neglects the free volume contribution [22]. The variation of the total free energy of mixing and its different contributions and corresponding phase diagrams as a function of temperature and composition will be estimated and used to interpret the miscibility behaviour of these blends.

2. Experimental

2.1. Synthesis and characterization of copolymers

Random copolymers of poly (isobutyl methacrylate-co-4-vinylpyridine) containing 20 mol% of 4-vinylpyridine(IBM4VP20) and poly (styrene-co-acrylic acid) containing 27 or 32 mol% of acrylic acid (SAA27 or SAA32) were prepared by solution free radical polymerization at 60 °C using azobis-isobutyronitrile (AIBN) as the initiator, keeping the conversion low. The copolymers were purified by two dissolution/reprecipitation cycles and dried under vacuum for several days.

The styrene (S) and 4-vinylpyridine (4VP) contents in the SAA, and IBM4VP copolymers were determined as previously described [14,17] by elemental analysis, UV spectroscopy, and proton NMR.

The weight average molecular weight M_w and the number average molecular weight M_n of SAA copolymers were determined by GPC using a Water HPLC while IBM4VP20 was characterized by viscometry only. The degree of polymerization (DP) of this copolymer was roughly estimated from viscometry.

The results of these characterizations and the glass transition temperature of these copolymers obtained by DSC traces are summarized in Table 1.

2.2. DSC measurements

The glass transition temperatures (Tgs) of the pure components and of their mixtures of different ratios as blends or complexes were determined with a Perkin Elmer DSC-7 Differential Scanning Calorimeter at a heating rate of 20 K/min within the temperature range 25–180 °C. Second scans to obtain reproducible values were carried and the Tg was taken as the mid point of the heat capacity change.

2.3. Thermal degradation studies

The TGA thermograms of the as cast and without any thermal pre-treatment copolymers and of their complexes were determined under nitrogen using TA instrument TGA 2590 thermogravimetric analyser at a heating rate of 10 °C/min from room temperature to 500 °C.

2.4. FTIR measurements

Thin films of the SAA27 and IBM4VP20 copolymers and of their SAA27/IBM4VP20 blends for FTIR measurements were prepared by casting from a 2–3% (w/v) solution in THF onto KBr disks. The solvent was first evaporated at room temperature. The disks were then dried in a vacuum oven at 60 °C for several days.

All infrared measurements were recorded on heating from room temperature to 180 °C above the Tgs' of the constituents and of their corresponding materials and then on cooling on a Nicolet 560 FTIR spectrometer with a spectral resolution of 2 cm^{-1}. Sixty scans were signal averaged. All the spectra were recorded after the same stabilization time. The quantitative study that concerns blends cast from THF was carried out at temperatures above Tg using a microprocessor-temperature and processor controller Omega CN3201.

3. Results and discussion

3.1. Complexation

When IBM4VP20 is mixed together with acidic copolymer SAA27, homogeneous solutions were obtained when THF was the common solvent. However, a precipitation occurred with all binary SAA27/IBM4VP20 mixtures over the entire feed composition, when butan-2-one was used as the solvent. Butan-2-one has a weaker hydrogen bonding ability than THF and thus favors the formation of inter-polymer complexes. The instantaneously formed inter-polymer complexes as precipitates were isolated from the solution and then dried in a vacuum oven at 60 °C for several days to constant weight.

As previously seen in Fig. 1, the complex yield in the range of 40–89% first increases, goes through a maximum around 50% by weight of SAA27, then decreases as the content of SAA-27 in the feed composition increases.

Similar behaviour but with lower yields of inter-polymer complexes in the range 35–63%, varying very slightly with the initial feed composition and a maximum practically constant within a

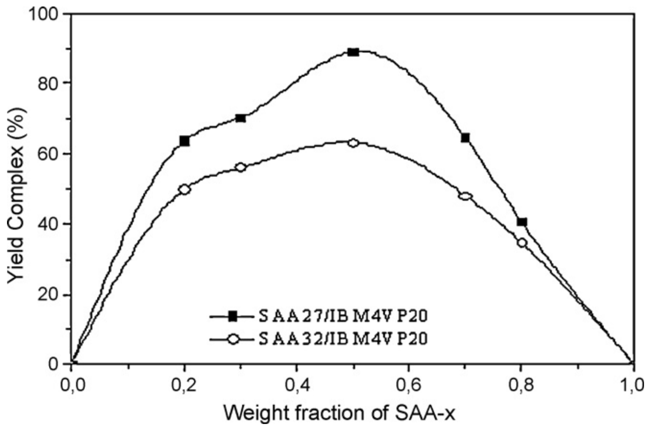

Fig. 1. Illustration of yield versus feed composition for SAA27/IBM4VP20 and SAA32/IBM4VP20 complexes.

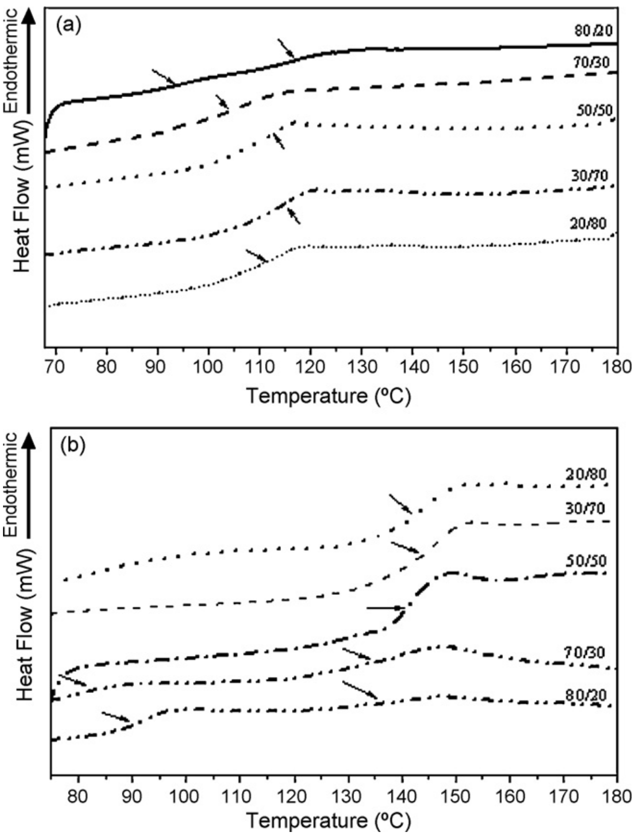

Fig. 2. (a) Thermograms of SAA27, IBM4VP20 and of their complexes of different ratios. (b) Thermograms of SAA32, IBM4VP20 and of their complexes of different ratios.

broader range as shown in the same Fig. 1, was observed in butan-2-one when the same basic IBM4VP20 is mixed with SAA32, an acidic copolymer containing a higher content of carboxylic groups though this latter copolymer is expected to develop a higher number of specific interactions. In agreement with previous results [17], this may be due to a more important self-association effect as the density of carboxylic groups increases within the acidic copolymer.

3.2. *Thermal analysis*

Fig. 2(a and b) shows DSC traces of the phases containing the isolated precipitates of SAA27/IBM4VP20 and SAA32/IBM4VP20 systems. Depending on the initial feed composition, one or two *Tg*s are observed with the precipitates of both systems.

The single *Tg* observed with phases (inter-polymer complexes) containing an initial feed of less than 70% by weight of SAA27 deviated positively from the weight average of their constituents and varied slightly with the initial weight fraction of SAA27. Within experimental error, the highest *Tg* value is observed with the complex (phase) of highest yield while the highest positive deviation is observed with the initial mixture containing 20% by weight of SAA27. Such positive deviation decreases progressively as the initial feed of SAA27 increased in the mixture until the observation of two *Tg*s. Fig. 3 illustrates the Tg-composition of this system.

Heterogeneous phases characterized by very broad transitions or two *Tg*s different from those of the two copolymers however observed with phases (precipitates) obtained from initial feed composition containing an excess of SAA27 and that led to relatively low complexation yield only, may interpret the formation of various complexes of different structures [23]. Several factors particularly the nature of solvent, the density, strength and accessibility of the interacting species, self-association and optimization of these inter-polymer interactions indeed affect the complexation phenomenon [11,24]. The accessibility of the interacting species itself is affected by the size of the side groups, the flexibility of the polymer chains and the dilution of these groups by inert moieties along the chains [25].

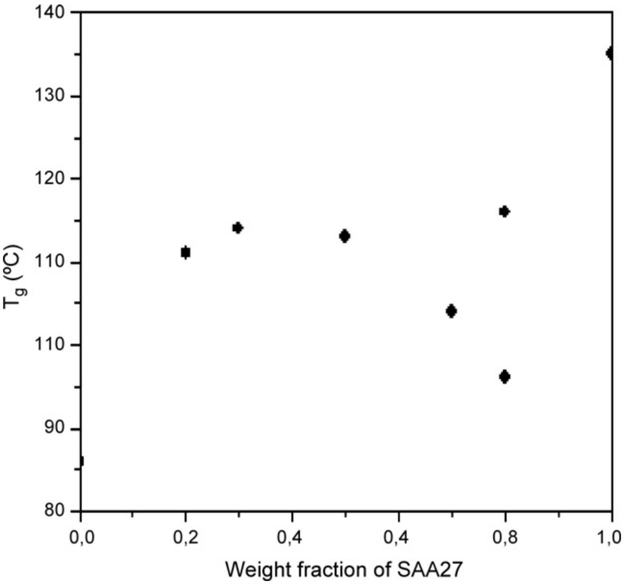

Fig. 3. Variation of the *Tg* of SAA27/IBM4VP20 mixtures with SAA-27 composition.

The *Tg* of highest value may be attributed to the formation of “ladder-like” complex of more compact structure while the lowest *Tg* could indicate the formation of inter-polymer complexes of looser structure resulting from a lower number of interacting sites.

Similarly, a single phase with a high *Tg* value is observed with SAA32/IBM4P20 isolated precipitates containing an initial feed of less than 50% by weight of SAA32, while two *Tg*s attributed as for the former system to heterogeneous phases were observed with phases obtained from initial feed composition containing an excess of SAA32. As the SAA32 composition increases, the phase of lower *Tg* is more pronounced in agreement with the observed low complexation yield.

A thermogravimetric analysis of these complexes was also carried out. Fig. 4(a and b) illustrates the TG and d(TG) curves of the copolymers and their different complexes while Table 2 summarizes their thermogravimetric data. Due to the specific interactions that occurred between SAA27 and IBM4VP20, these complexes exhibited a significant improved thermal stability. Indeed, the T_{onset} and the Td_{max} of the isolated precipitates are higher than those of the pure constituents. A very small loss of water less than 1% by weight is observed in the 25–180 °C temperature range.

In agreement with the DSC results, one-step degradation only, with a Td_{max} at 381 °C, higher than that of IBM4VP20 and one of the weight average of both constituents of the complex,

Table 2
Thermogravimetric data of SAA27, IBM4VP20 and of their complexes in butan-2-one.

Composition	Td_1 (°C)	Td_2 (°C)	T_{onset} (°C)	Td_{max} (°C)
0/100	353	–	233	353
20/80	–	381 402	235	381
30/70	–	414	270	414
50/50	–	415	275	415
70/30	–	418	277	418
80/20	–	420	278	420
100/0	–	405	270	405

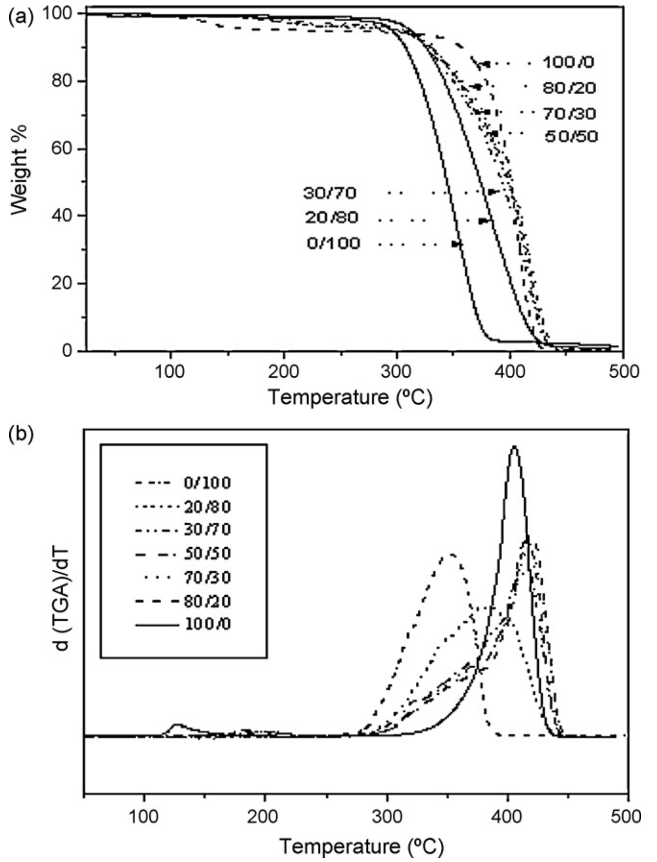

Fig. 4. TGA (a) and d(TGA)/dT (b) curves of SAA27, IBM4VP20 and their complexes of different ratios.

is observed with the homogeneous 20/80 isolated precipitate. However, two-step degradation temperatures appeared in the 300–500 °C temperature range with heterogeneous isolated precipitates obtained from initial mixtures containing higher amount of SAA27 and that showed broad transitions or two *Tg*s. The shift to higher temperature of the $Td_{\max}$ of their second step of degradation is an evidence of their improved thermal stability.

3.3. FTIR analysis

At equilibrium, above the glass transition temperatures of the copolymers and below the onset of degradation of these latter and of their mixtures, FTIR spectroscopy is used in a first step to evidence the existence of hydrogen bonding in the blends and then to analyze quantitatively the interactions that occurred within the SAA27 copolymer and between the two components within the blends upon mixing SAA27 with IBM4VP20. Fig. 5 displays an example of FTIR spectra of SAA27/IBM4VP20 blends recorded at 25 °C from which PS contribution was subtracted. As it is shown in this figure, IBM4VP20 (0/100) shows a strong peak in this region at 1597 cm^{-1} characteristic of free pyridine. The intensity of this peak decreases progressively as SAA27 is added to the blend and a new band attributed to associated pyridine appeared at 1606 cm^{-1}. It is worth noting the absence of pyridinium ions that usually appear in this region at around 1637–1640 cm^{-1} [26,27].

The expected hydrogen bonding interactions within the SAA27 copolymer and the blends are described by Schemes 1–3.

Since IBM4VP20 contains both carbonyl and nitrogen groups, the expected hydrogen bonds that this latter may form with SAA27 are described by Schemes 2 and 3.

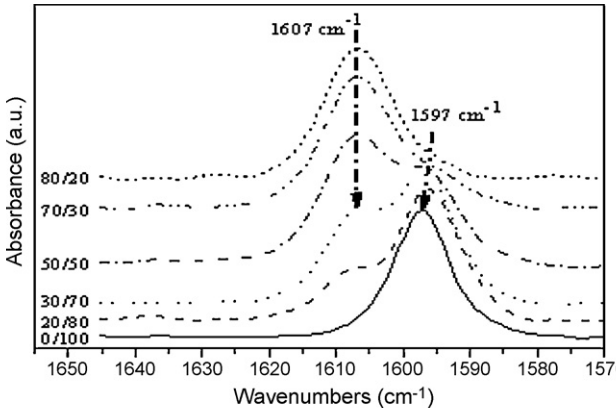

Fig. 5. Scale-expanded infrared difference spectra (subtraction of polystyrene) of SAA27/IBM4VP20 blends in the 1650–1570 cm^{-1} region recorded at 25 °C.

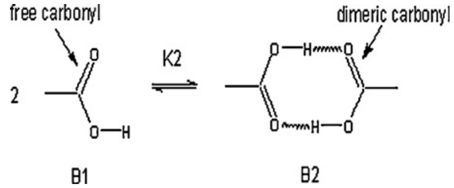

Scheme 1.

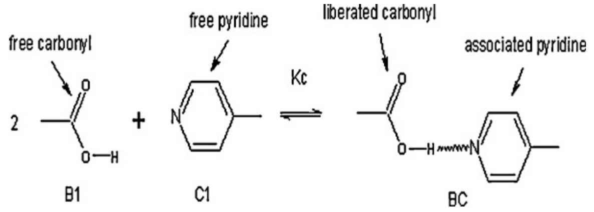

Scheme 2.

The carboxyl–pyridine inter-association interactions that occurred between SAA27 and IBM4VP20 within this system are stronger than carboxyl–carboxyl dimerization. Similar results are reported in the literature [26,27].

The self-association equilibrium constant K_2 of SAA27, previously determined [14,17] and the inter-association equilibrium constant K_A are given by:

$$K_2 = \frac{\phi_{B_2}}{\phi_{B_1}^2}\left[\frac{1}{2}\right] \tag{1}$$

$$K_A = \frac{\phi_{BA}}{\phi_{B_1}\phi_{A_1}}\left[\frac{r}{1+r}\right] \tag{2}$$

and the stoichiometry of the system:

$$\phi_{B_1} + \phi_{B_2} + \phi_{A_1} + \phi_{BA} = 1 \tag{3}$$

$$\Phi_B = \phi_{B_1}\left[1 + \frac{K_A\phi_{A_1}}{r}\right] + 2K_2\phi_{B_1}^2 \tag{4}$$

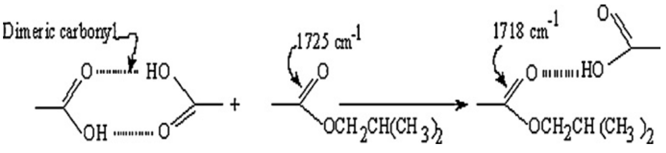

Scheme 3.

Table 3
Curve fitting data from infrared spectra of SAA27/IBM4VP20 blends in the 1650–1550 cm^{-1} region on heating from 130 °C to 180 °C and on cooling from 180 °C to 150 °C.

	T (°C)	F_f	F_{ass}	φ_{A1}	T (°C)	F_f	F_{ass}	φ_{A1}
70/30	130	0.60	0.40	0.18	180	0.71	0.29	0.21
	140	0.61	0.39	0.18	170	0.69	0.31	0.21
	150	0.63	0.37	0.19	160	0.68	0.32	0.20
	160	0.64	0.36	0.19	150	0.65	0.35	0.19
	170	0.67	0.33	0.20	140	0.64	0.36	0.19
	180	0.68	0.32	0.20	130	0.63	0.37	0.19
	130	0.69	0.31	0.35	180	0.82	0.18	0.41
	140	0.71	0.29	0.35	170	0.81	0.19	0.41
50/50	150	0.72	0.28	0.36	160	0.78	0.22	0.38
	160	0.76	0.24	0.38	150	0.76	0.24	0.38
	170	0.76	0.24	0.38	140	0.75	0.25	0.37
	180	0.78	0.22	0.40	130	0.74	0.26	0.37
	130	0.81	0.19	0.57	180	0.90	0.10	0.63
	140	0.83	0.17	0.59	170	0.89	0.11	0.63
30/70	150	0.84	0.16	0.59	160	0.89	0.11	0.62
	160	0.84	0.16	0.59	150	0.89	0.11	0.62
	170	0.84	0.16	0.59	140	0.88	0.12	0.62
	180	0.85	0.15	0.60	130	0.88	0.12	0.61

$$\Phi_A = \phi_{A_1}(1 + K_A\phi_{B_1}) \quad (5)$$

where ϕ_i, Φ_i and r are the volume fractions of the polymer segment containing the i species, volume fraction of interacting polymer in the blend and the ratio of the molar volumes V_A/V_B respectively, while the index B and A relates to self-associated polymer (B) which can inter-associates with polymer (A), respectively.

Based on our previous results [13,17] that confirmed by DSC and IGC (inverse gas chromatography) the immiscibility of poly (styrene-co-acrylic acid) containing up to 32 mol% of acrylic acid with PIBMA as mainly due to steric effect, we assumed that the carbonyl groups of IBM4VP20 inter-associate weakly with the acidic SAA27. Yet Coleman et al. [28] reported in their study of poly (n-butyl methacrylate-co-4-vinylphenol)/poly (styrene-co-2-vinylpyridine) blends that the fraction of hydrogen-bonded carbonyl groups increases with the temperature. Neglecting this contribution, an analysis of the interactions of only hydrogen bonding type that occurred between the two components of the mixture that considers the carboxyl–pyridine interactions described only by Scheme 2, was carried out in the 1650–1550 cm^{-1} region, using adequate spectral curve fitting procedures to determine the fractions of the relative areas of the free and associated pyridine from the equation below, with F_f, *the* fraction of the free pyridine such as:

$$F_f = \frac{A_f^{\text{pyridine}}}{A_f^{\text{pyridine}} + A_{\text{ass}}^{\text{pyridine}}} \quad (6)$$

where A is the area of the bands at 1607 cm^{-1} and 1597 cm^{-1} attributed to the associated and free pyridine respectively assuming an absorptivity ratio of 1 [28].

The curve fitting data from FTIR spectra of SAA27/IBM4VP20 blends as cast from THF at different compositions carried out in this region on heating and cooling from 180 °C to 130 °C are shown in Table 3.

These results show that the fraction of associated pyridine increases with the SAA27 composition in the blend, decreases as the temperature is raised in this range and then increases upon cooling to lower temperature with an observed hydrogen bonding recovery less than the initial one that may be attributed, in addition to polymer chain rearrangements, to the cooling process carried out in the FTIR experiment that takes longer time than the DSC one. Some differences are therefore expected in the results as obtained by these two techniques.

Band separation in the 1800–1650 cm^{-1} carbonyl region is difficult to carry out due to the significant overlapping of the different species.

3.4. Thermodynamic analysis

A thermodynamic analysis using the Painter–Coleman association model is performed [18].

The inter-association equilibrium constant K_A and the enthalpy of hydrogen bonding formation of SAA27/IBM4VP20 blends are calculated from the data shown in Tables 3 and 4 and Fig. 6

Using the appropriate polymer characteristics and the standard equilibrium constants K_2 and K_A given in Table 4, we calculated the variation of the total free energy of mixing and its different contributions and corresponding phase diagrams as a function of temperature and composition.

According to this model, the free energy of mixing of two polymers when hydrogen bonding interactions are present is expressed by:

$$\frac{\Delta G_M}{RT} = \frac{\Phi_A}{M_A}\ln\Phi_A + \frac{\Phi_B}{M_B}\ln\Phi_B + \Phi_A\Phi_B\chi_{AB} + \frac{\Delta G_H}{RT} \quad (7)$$

The Flory-Huggins parameter χ is given by

$$\chi = (\delta_A - \delta_B)^2\frac{V_{\text{ref}}}{RT} \quad (8)$$

where δ_i is the solubility parameter which can be determined by group molar contribution.

The term $\Delta G_H/RT$ is the favourable contribution to the change in the free energy of mixing due to the presence of intermolecular hydrogen bonding interactions and is given by

$$\frac{\Delta G_H}{RT} = \Phi_B\ln\left(\frac{\phi_{B_1}}{\phi_{B_1}^0}\right) + \frac{\Phi_A}{r}\ln\phi_{A_1} + \Phi_B[\phi_{B_1}^0(1 + K_2\phi_{B_1}^0)] - \phi_{B_1}(1 + K_2\phi_{B_1}) - \left[\frac{\Phi_B}{\bar{h}^0}\ln\Phi_B + \frac{\Phi_A}{r}\ln\Phi_A\right] \quad (9)$$

Table 4
Polymer characteristics and the standard equilibrium constants K_2 and K_A.

$K_2 = 1270$	$h_B = -6.46$	$V_B = 38$	$V_{\text{styrene}} = 94$	$\delta_B = 11.7$	$\delta_{\text{styrene}} = 9.5$
$K_A = 5800$	$h_A = -11.0$	$V_A = 85$	$V_{\text{IBM}} = 135.1$	$\delta_A = 10.85$	$\delta_{\text{IBM}} = 8.6$

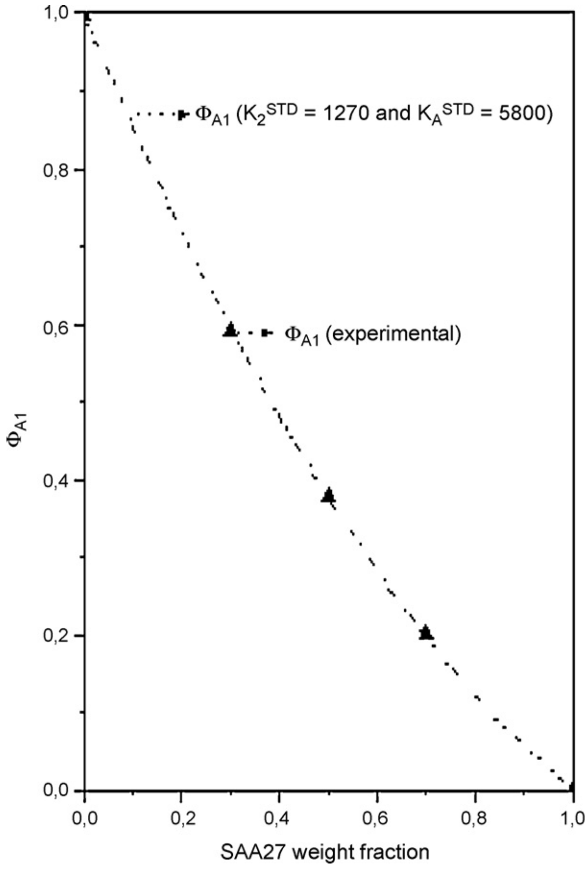

Fig. 6. Experimental and theoretical volume fractions of free pyridine in the SAA27/IBM4VP20 system versus blend composition at 170 °C.

where

$$\overline{h}^0 = \frac{1 + 2K_B\phi^0_{B_1}}{1 + K_B\phi^0_{B_1}}$$

Taking into account the intramolecular screening factor 'γ' assumed to be 0.20, the free energy of mixing of two polymers when hydrogen bonding interactions are present is expressed by [22]:

$$\frac{\Delta G_M}{RT} = \frac{\Phi_A}{N_A}\ln\Phi_A + \frac{\Phi_B}{N_B}\ln\Phi_B + (1-\gamma)\Phi_A\Phi_B\chi_{AB} + \frac{\Delta G_H}{RT} \qquad (10)$$

and

$$\Phi_B = \phi_{B_1}\left[1 + \frac{\tilde{K}_A\phi_{A_1}}{r}\right] + 2\tilde{K}_2\phi^2_{B_1} \qquad (11)$$

$$\Phi_A = \phi_{A_1}(1 + \tilde{K}_A\phi^2_{B_1}) \qquad (12)$$

$$\tilde{K}_2 = K_2\frac{\gamma + (1-\gamma)\Phi_B}{\Phi_B} \qquad (13)$$

$$\tilde{K}_A = K_A(1-\gamma) \qquad (14)$$

Fig. 7 illustrates an example of these variations at 25 °C. As it can be seen in this figure, the main contribution at this temperature is due to the $\Delta G_H/RT$ term related to specific interactions. The negative value of $\Delta G_M/RT$ and the positive second derivative observed for less than 70% of SAA27 in the blend suggest that these blends are miscible at this temperature in this composition range.

Because the equilibrium constants K_2 and K_A are temperature dependent, obeying the well known van t'Hoff equation, the free energy of mixing can be determined at different temperatures.

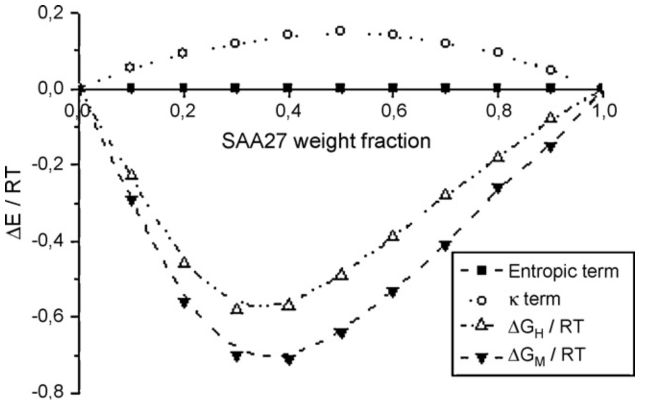

Fig. 7. Total free energy and its different contributions as a function of SAA27/IBM4VP20 blend composition at 25 °C using $K_2^{STD} = 1270$ and $K_A^{STD} = 5800$.

Fig. 8 shows the variation of some $\Delta G_M/RT$ with temperature of the SAA27/IBM4VP20 blend system.

Accordingly, the miscibility of this system decreases with temperature leading to phase separation at high temperatures. Indeed the fraction of associated pyridine characterizing the inter-polymer interactions decreased with the temperature. With the expected trend of variation, the theoretical results are in a fair agreement with the experimental observations. This may be due to the accessibility of the functional groups that is affected by bulky side groups among others, not considered in this case and to the neglected contribution from the eventual carboxyl–ester interactions that may occur between particularly as the temperature is raised and as reported by Coleman et al. [28]. It is also worth noting that the theoretical equation describing the free energy of mixing does not consider the free volume effect. The resulting inter-association equilibrium constant that does not take into account such effects is underestimated.

The spinodal phase diagram is obtained from the second derivative of the free energy with respect to Φ_B as the conditions for a binary blend to be thermodynamically miscible are:

$$\frac{\Delta G_M}{RT} < 0 \quad \text{and} \quad \frac{\partial^2}{\partial\Phi_B^2}\Delta G_M > 0$$

Fig. 9 shows the theoretical phase diagram of the SAA27/IBM4VP20 blend system. A lower critical solution temperature (LCST) occurs at relatively high temperature thus partial miscibility is observed for this system. This behaviour is mainly due, besides the effects of errors in the estimation of the solubility

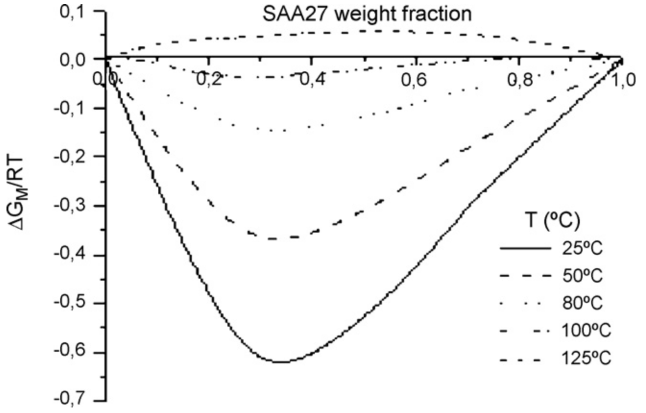

Fig. 8. Total free energy as a function of SAA27/IBM4VP20 blend composition at different temperatures using $K_2^{STD} = 1270$, $h_B = -6.46$ kcal/mol, $K_A^{STD} = 5800$ and $h_A = -11$ kcal/mol.

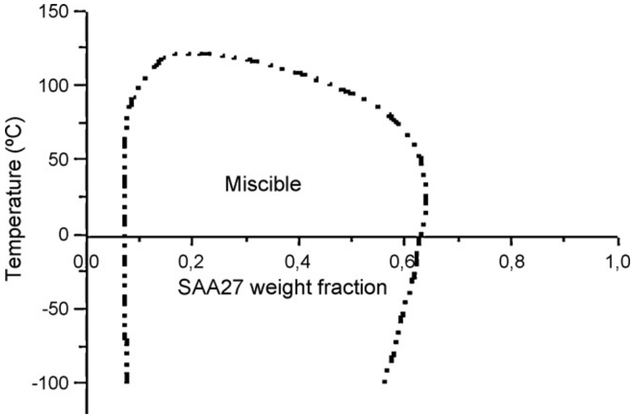

Fig. 9. Temperature effect on the miscibility of the SAA27/IBM4VP20 blend system.

parameter values and enthalpy of hydrogen bonding formation, as mentioned above, to the several factors that underestimate the inter-association equilibrium constant that became weak at high temperature.

4. Conclusion

The investigation of the miscibility and hydrogen bonding interactions that occurred between poly (isobutyl methacrylate-co-4-vinylpyridine) containing 20 mol% of 4-vinylpyridine (IBM4VP20) and poly (styrene-co-acrylic acid) containing 27 mol% of acrylic acid (SAA27), examined by DSC, TGA and FTIR spectroscopy qualitatively and quantitatively in the 25–180 °C temperature range, showed that sufficient density of specific carboxyl–pyridine interactions occurred within this system and led to miscible blends as cast from THF and to various inter-polymer complexes of significantly improved thermal stability when butan-2-one is the common solvent. Due to self-association effect, increasing the carboxylic content above 27 mol% as with SAA32, led to lower complexation yields.

The thermodynamic analysis of the specific interactions of hydrogen bonding type within this system, using the Painter–Coleman association model that considers the screening effects and neglects not only the contribution of the weak carboxyl–ester interactions due to bulky groups but also other effects, predicted from the variation of the total free energy of mixing and its different contributions a phase behaviour in a fair agreement with the experimental results. A partial miscibility is observed when the SAA27 is in excess.

References

[1] J.V. Gasa, R.A. Weiss, M.T. Shaw, J. Membr. Sci. 320 (1–2) (2008) 215–223.
[2] A. Habi, S. Djadoun, Thermochim. Acta 469 (2008) 1–7.
[3] X.F. Luo, X. Hu, X.Y. Zhao, S.H. Goh, X.D. Li, Polymer 44 (18) (2008) 5285–5291.
[4] J.A. Lima, M.I. Felisberti, Eur. Polym. J. 44 (4) (2008) 1140–1148.
[5] L. Goitisolo, J.J. Eguiazabal, J. Nazabal, Eur. Polym. J. 44 (7) (2008) 1978–1987.
[6] S.W. Kuo, Polymer 49 (2008) 4420–4426.
[7] L. Zhu, M. Jiang, L. Liu, H. Zhou, L. Fan, Y. Zhang, J. Macromol. Sci. Phys. B37 (6) (1998) 805–826.
[8] Y. He, B. Zhu, Y. Inoue, Prog. Polym. Sci. 29 (2004) 1021–1051.
[9] H.R. Motzer, P.C. Painter, M.M. Coleman, Macromolecules 34 (2001) 8388–8389.
[10] N. Abdellaoui, S. Djadoun, J. Appl. Polym. Sci. 98 (2005) 658–664.
[11] S. Viswanathan, M.D. Dadmun, J. Polym. Sci. Part B: Polym. Phys. 42 (2004) 1010–1022.
[12] G.R. Brannock, J.W. Barlow, D.R. Paul, J. Polym. Sci. Part B: Polym. Phys. 28 (1990) 871–891.
[13] F. Feraz, A.S. Hadj Hamou, S. Djadoun, Eur. Polym. J. 31 (7) (1995) 665–669.
[14] A.S. Hadj Hamou, S. Djadoun, J. Appl. Polym. Sci. 103 (2007) 1011–1024.
[15] E. Eastwood, S. Viswanathan, C.P. O'Brien, D. Kumar, M.D. Dadmun, Polymer 46 (2005) 3957–3970.
[16] A. Rasheed, H.G. Chae, S. Kumar, M.D. Dadmun, Polymer 47 (2006) 4734–4741.
[17] K. ElMiloudi, A.S. Hadj Hamou, S. Djadoun, Polym. Eng. Sci. 48 (2008) 458–466.
[18] M.M. Coleman, J.F. Graf, P.C. Painter, Specific interactions and the Miscibility of polymer blends, Technomic Publishing, Lancaster, PA, 1991.
[19] J.A. Pomposo, M. Cortazar, E. Calahorra, Macromolecules 27 (1994) 245–251.
[20] C.S. Cleveland, K.S. Guigley, P.C. Painter, M.M. Coleman, Macromolecules 33 (2000) 4278–4280.
[21] S.W. Kuo, C.L. Lin, F.C. Chang, Polymer 43 (2002) 3943–3949.
[22] M.M. Coleman, P.C. Painter, Prog. Polym. Sci. 20 (1995) 1–59.
[23] M. Jiang, M. Li, M. Xiang, H. Zhou, Adv. Polym. Sci. 146 (1999) 121–196.
[24] R.B. Radmard, M.D. Dadmun, Polymer 42 (2001) 1591–1600.
[25] M.M. Coleman, P.C. Painter, Macromol. Chem. Phys. 199 (1998) 1307–1314.
[26] K. ElMiloudi, S. Djadoun, J. Polym. Sci. Part B: Polym. Phys. 47 (2009) 923–931.
[27] V. Villar, L. Irusta, M.J. Fernandez-Beridi, J.J. Iruin, M. Iriarte, L. Gargallo, D. Radie, Thermochim. Acta 402 (2003) 209–218.
[28] M.M. Coleman, L.A. Narvett, P.C. Painter, Polymer 39 (1998) 5867–5869.